# Tension and Compression in the Cytoskeleton of PC-12 Neurites II: Quantitative Measurements

**T. J. Dennerll, H. C. Joshi, V. L. Steel, R. E. Buxbaum,* and S. R. Heidemann**

Department of Physiology and *Department of Chemical Engineering, Michigan State University, E. Lansing, Michigan 48824

***Abstract.*** We assessed the mechanical properties of PC-12 neurites by applying a force with calibrated glass needles and measured resulting changes in neurite length and deflection of the needle. We observed a linear relationship between force and length change that was not affected by multiple distensions and were thus able to determine neurite spring constants and initial, nondistended, rest tensions. 81 out of 82 neurites showed positive rest tensions ranging over three orders of magnitude with most values clustering around 30–40 μdynes. Treatment with cytochalasin D significantly reduced neurite rest tensions to an average compression equal to 14% of the former tension and spring constants to an average of 17% of resting values. Treatment with nocodazole increased neurite rest tensions to an average of 282% of resting values but produced no change in spring constant. These observations suggest a particular type of complementary force interaction underlying axonal shape; the neurite actin network under tension and neurite microtubules under compression. Thermodynamics suggests that microtubule (MT) assembly may be regulated by changes in compressive load. We tested this effect by releasing neurite attachment to a polylysine-coated surface with polyaspartate, thus shifting external compressive support onto internal elements, and measuring the relative change in MT polymerization using quantitative Western blotting. Neurons grown on polylysine or collagen without further treatment had a 1:2 ratio of soluble to polymerized tubulin. When neurites grown on polylysine were treated with 1% polyaspartate for 15–30 min, 80% of neurites retracted, shifting the soluble: polymerized tubulin ratio to 1:1. Polyaspartate treatment of cells grown on collagen, or grown on polylysine but treated with cytochalasin to reduce tension, caused neither retraction nor a change in the soluble:polymerized tubulin ratio. We suggest that the release of adhesion to the dish shifted the compressive load formerly borne by the dish onto MTs causing their partial depolymerization. Our observations are consistent with the possibility that alterations in MT compression during growth cone advance integrates MT assembly with the advance.

SINCE the pioneering studies of Yamada et al. (59), many investigators have found a clear cut "division of labor" in the role of the cytoskeleton in growth cone motility and axonal elongation. Anti-microtubule (MT)[1] drugs cause neurites to collapse but have no effect on growth cone motility functions, e.g. ruffling, microspike activity, etc. (8, 17, 24, 30, 31, 49). Conversely, anti-actin drugs inhibit growth cone motility functions but neurites remain extended (8, 24, 31, 49). Further, drugs that disrupt the actin network stabilize the neurite to retraction, while drugs that disrupt MTs cause retraction. Also, drugs that augment actin assembly cause retraction while drugs that augment MT assembly stabilize neurites to retraction and sometimes cause extension (15, 31, 35, 49). Similarly, the networks move at different rates in slow axonal transport (4). Apparently, while MT-based and actin-based elements of neuronal growth interact, they are structurally and functionally distinct (34).

Neurites of cultured neurons have been shown by indirect means to be under tension (5, 31). Bray (6) elicited apparently normal neurite elongation by "towing" neurites with an appropriately paced motor in a process very similar to the "towed growth" long known to occur in situ (57). Tension has also been shown to markedly alter the motility at the edge of fish skin cells (32), align the division plane of plants (36) and dramatically orient growing chick myofibers (55). These and other examples (53) of mechanical force affecting cell growth, shape, and polarity, processes widely regarded to depend on cytoskeletal function (1, 18), suggest that tension may play a role in regulating the cytoskeleton. Previous results from our lab (31) caused us to propose that actin and MTs in PC-12 neurites are in a complementary force interaction: the actin network being under tension that is partly supported by MT compression and partly supported by the underlying substrate. This postulated complementary force

1. *Abbreviations used in this paper*: Cal, calibration constant; Cyt-D, cytochalasin D; MT, microtubule; MTP, microtubule protein; NGF, nerve growth factor; NOC, nocodazole.

interaction, similar to the interaction of structural elements in "tensegrity" architecture (21), provides, in principle, a means for integrating MT assembly with the advance of the growth cone.

In an effort to better understand the structural roles of actin and MTs in axonal shape and to test our complementary force model, we directly measured mechanical force in PC-12 neurites and the effect of cytoskeletal drugs on that force. We have also measured changes in the ratio of soluble and polymerized tubulin before and after neurite retraction.

## Materials and Methods

### Sources

Nocodazole (NOC) was obtained from Aldrich Chemical Co., Inc. (Milwaukee WI). Cytochalasin D (Cyt-D) DMSO, polyaspartate, EHNA, trypsin, fish gelatin, BSA, peroxidase-conjugated goat anti-rabbit IgG, and diaminobenzidine were obtained from Sigma Chemical Co. (St. Louis, MO). Chromel wire was obtained from Omega Engineering, Inc. (Stamford, CT). $Ca^{++}$ and $Mg^{++}$ free PBS and FCS was obtained from Gibco (Grand Island, NY). Sequannal grade SDS was obtained from Pierce Chemical Co. (Rockford, IL). Nitrocellulose was obtained from Scheicher & Schuell (Keene, NH). Rabbit anti-mouse IgM was obtained from Miles Laboratories (Naperville, IL).

### Neurite Tension Measurements

PC-12 cells were grown as previously described (31), primed in 50 ng/ml 7s nerve growth factor (NGF) for 4–6 d, then replated on untreated 60-mm tissue culture dishes in 7s NGF media, allowing neurites to regenerate for 2–3 d before tension measurements. The microscope was mounted on a vibration isolation table and cultures were maintained at 37°C on the microscope stage with a Sage Instruments air curtain incubator. NOC and Cyt-D stock solutions were prepared at 1,000× concentration in DMSO, with final experimental concentrations of 1 μg/ml NOC and 2 μg/ml Cyt-D with 0.1% DMSO for each. Neurite tensions were measured (see below) both before and 10–15 min after addition of drug. Only those neurites that remained attached throughout an experimental series of deflections could be analyzed for the effect of the drug. Drug-treated neurites showed length changes of less than 5%, generally less than 1%. Control experiments were done in a similar manner in 0.1% DMSO.

Glass needles were fabricated and calibrated for force as described by Nicklas (41), with the following modifications. Two relatively stiff "reference" needles were made from 8- and 16-mm lengths of uniform diameter 25 μm chromel wire. Each was calibrated for force by hanging weights from their tips. A third 24-mm wire needle could then be calibrated indirectly by using the following standard relation from beam theory:

$$\text{Force} = \frac{(\text{constant})\ (\text{tip displacement})}{(\text{needle length})^3}.$$

Values obtained for the constant from the two shorter (stiffer) needles differed by less than 1% and gave a calculated value of 90.9 μdynes/μm deflection for the third needle. More flexible glass needles were then calibrated by bending them against this wire needle, and subsequently glass needles against each other, to get "working" needles with stiffness calibration constants (Cal) of 1–10 μdynes/μm.

To make a tension measurement, a force calibrated needle is placed at the center of the neurite and rapidly moved perpendicular to the neurite axis, using a Narishige hydraulic micromanipulator, causing both neurite distension and needle deflection (see Fig. 1). After holding for 2–3 s, the needle is lifted; both needle and neurite assume rest positions almost instantaneously. This procedure is repeated 10 to 20 times at various displacements in random order. Video recording allows direct measurement from the video screen of neurite rest length ($L_o$), lateral neurite displacement ($b$), and needle deflection ($d$) for each "pull." Screen measurements were converted into actual distances through the use of a stage micrometer. These values were used to calculate axial neurite stretch tension ($T_s$) in microdynes and corresponding neurite stretch lengths ($L_s$) for each pull by the following analysis: Since $c^2 = a^2+b^2$, $L_s = 2c = 2\ (a^2+b^2)^{1/2}$. A vector force balance is then used to determine axial forces in the stretched neurite:

$T_s = T_o+k_1\ (L_s-L_o)$ = force parallel to neurite
$d\ (Cal)$ = force perpendicular to neurite
$d(Cal) = 2\sin\theta\{T_o+k_1\ (L_s-L_o)\}$
$\sin\theta = b/c = 2b/L_s$ — $T_s$ = neurite tension at length $L_s$
$d(Cal) = 4b\{T_o+k_1\ (L_s-L_o)\}/L_s$ — $T_o$ = neurite rest tension
$d(Cal)L_s/4b = T_o+k_1\ (L_s-L_o)$ — $k_1$ = neurite spring constant.

Distended neurite axial tension $d(Cal)L_s/4b$ is plotted as a function of change in neurite length $(L_s-L_o)$. Linear plots indicate Hookian elastic behavior where the y-intercept equals the neurite rest tension ($T_o$, tension at 0 distension) and the slope equals the spring constant ($k_1$).

### Retraction of Neurites in Response to Surface Active Treatments

PC-12 cells were grown as previously described (24) for 6 d in NGF media changed every other day. Cells were replated in NGF-containing medium onto 150-mm tissue cultures dishes treated with 0.1% polylysine or onto dishes coated with rat tail collagen (23) and allowed to grow for an additional 6 d with fresh medium every other day. The number of neurites before and after experimental treatments was assessed by the method previously described (24). Briefly, small regions of the tissue culture dish were circled, photographically surveyed before and after treatment and the number of neurites counted from the photographs. 1 h before the experiment the cells were rinsed with NGF medium (37°C) to remove cell debris and returned to the incubator. 30 min later cultures were circled and photographed as described above and incubated for an additional 30 min. Treatment began by decreasing the medium of the dishes to 2 ml and adding polyaspartate from a 10% stock made in NGF containing medium to a final concentration of 1%. Cyt-D (2 μg/ml) and EHNA (0.2 mM) were added from 1,000× stocks made in DMSO. The culture was gently rocked back and forth to insure mixing, re-incubated for 15–30 min and circled regions of the dish were again photographically surveyed. Medium was removed from the cultures and replaced with 2 ml of 0.25% trypsin dissolved in $Ca^{++}$ and $Mg^{++}$ free PBS. Treated cultures were incubated for 5 min and the circled regions were reviewed.

### Detergent Extraction of Cells

One 150-mm tissue culture plate containing 1–1.5 × $10^6$ cells was used for each experimental treatment of PC-12 cells as described for Table I. Soluble and polymerized cell extracts were obtained by a modification of the procedure of Drubin et al. (20). After 15–30 min in the presence of polyaspartate, cytochalasin, EHNA and trypsin, cultures were rinsed briefly with 0.1 M MES, pH 6.75, 1 mM $MgSO_4$, 2 mM EGTA, 0.1 mM EDTA, and 0.1 mM GTP. 2.0 ml of the above buffer containing the protease inhibitors mixture described by Drubin et al. (20), 2 M glycerol and 0.1% Triton X-100 were then added to the dish. This buffer has been shown to quantitatively separate assembled from unassembled tubulin (13, 20, 50). The culture dish was gently rocked and incubated at 37°C for 8 min. The Triton extract supernatant was centrifuged at 1,000 *g* for 3 min at room temperature to pellet any lifted cells. The supernatant of this spin was subjected to electrophoresis as the soluble fraction. The Triton-extracted cytoskeletal ghosts were then solubilized from the dish by addition of 2.0 ml of 0.5% SDS and scraping with a rubber policeman. This SDS extract was added to the pellet from the centrifuged Triton extract. The tube was vortexed for 30 s and the extract subjected to electrophoresis as the polymerized fraction. 20 μl of the Triton and SDS extracts from a single culture plate were subjected to electrophoresis and immunoblotted as described below. The need to pellet the DNA as described by Drubin et al. (20) was avoided by using Pierce Sequanal SDS (other types proved unsuitable for unknown reasons) and MES instead of Pipes in the SDS extraction buffer.

### Immunoblots

Samples of PC-12 extracts and of microtubule protein purified from beef brain were subjected to electrophoresis, transferred to nitrocellulose and probed with a monoclonal antibody to beta tubulin. Microtubule protein (MTP) was isolated in the presence of glycerol by the method of Weingarten et al. (56) with the modification that 0.1 M Pipes, at pH 6.6, was used instead of MES. MTP was further purified by chromatography on phosphocellulose by the method of Williams and Detrich (58). Purified proteins or PC-12 extracts were subjected to electrophoresis in adjoining lanes of a 10% SDS-polyacrylamide gel (33). After electrophoresis, the gel was electroblotted onto nitrocellulose using a Bio-Rad Trans-blot apparatus at 180 V for 5 h.

*Table I. Retractions of PC-12 Neurites in Response to Surface Active Reagents*

| Growth Surface | Treatment | Before* | After‡ | Retracted |
|---|---|---|---|---|
| | | | | % |
| Polylysine | PolyAsp ($n$ = 6) | 3,956 | 732 | 81 |
| Collagen | PolyAsp ($n$ = 3) | 1,459 | 1,403 | 4 |
| Collagen | Trypsin ($n$ = 1) | 725 | 56 | 92 |
| Polylysine | PolyAsp + Cyt-D ($n$ = 2) | 1,340 | 1,034 | 23 |

* Number of neurites in a circled region of the dish before experimental treatment.
‡ Number of neurites in the same circled region of the dish after experimental treatment (see Materials and Methods).

After rinsing the nitrocellulose twice for 10 min with PBS the membrane was "blocked" overnight with 3% fish gelatin, 2% BSA and 8% FCS in PBS. The membrane was rinsed briefly in PBS containing 0.1% Tween 20 (TPBS) and incubated with shaking at 37°C for 3 h with a monoclonal antibody to beta tubulin kindly provided by Dr. David Asai of Purdue University. The membrane was washed twice with 0.1% SDS, 0.5% Tween 20, 0.5% Nonidet P-40 in 0.5 M NaCl for 15 min with shaking followed by 2 washes of 10 min each with TPBS. The blot was subsequently incubated in rabbit anti-mouse IgM for 45 min and with peroxidase-conjugated goat anti-rabbit IgG for 45 min both with shaking at 37°C. The nitrocellulose was then rinsed as described above for the anti-tubulin antibody. Before adding substrate for peroxidase reaction, the membrane was rinsed 4× with PBS for 10 min each with shaking. 20 μl of 30% $H_2O_2$ and 20 mg of diaminobenzidine dissolved in 50 ml PBS were added to the membrane and the reaction allowed to proceed for 5 min. The nitrocellulose was rinsed 4× in water and dried for analysis. The HRP product bands on the nitrocellulose were measured by densitometry using a Zieneh or LKB 2222 laser densitometer. Blots scanned by both devices gave identical results.

## Results

### Tension Measurements

PC-12 neurites were multiply distended orthogonal to the neurite axis using a force calibrated glass needle to measure neurite mechanical properties (see Fig. 1 and Materials and Methods). Tensions were measured on 82 neurites and Fig. 2 shows the results for three typical tension experiments. Regression coefficients ($R$) of 0.80 or better were observed in over 90% of the neurite length-tension plots. Initial neurite

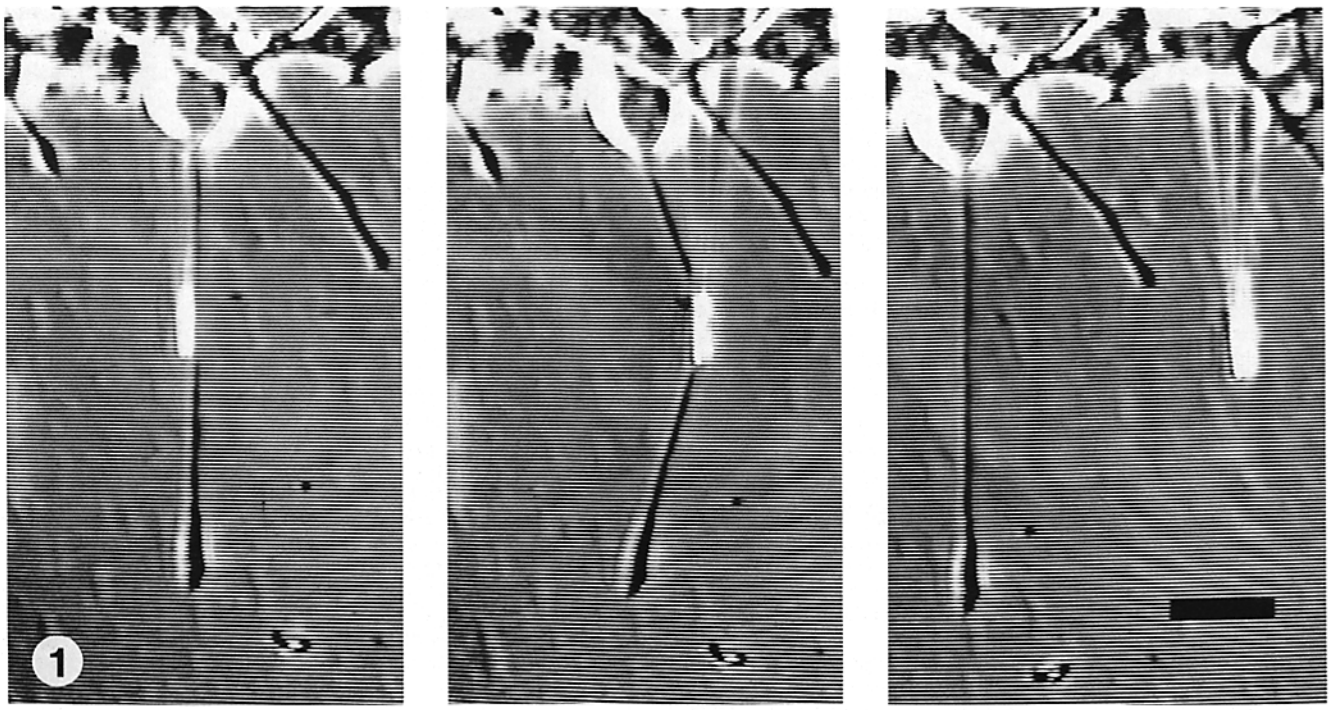


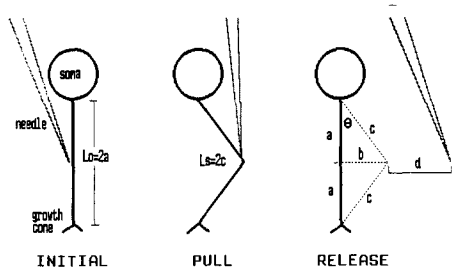


*Figure 1.* Measurement of neurite tension by lateral displacement. Method of tension measurement is shown in light micrographs (*top*) and cartoon illustration (*bottom*). After the experiment, measurements are made from recorded video images of neurite rest length ($L_o$), neurite lateral displacement ($b$) and force calibrated needle deflection ($d$). These measurements are used to calculate neurite axial tension and change in neurite length (see Materials and Methods). Bar, 20 μm.

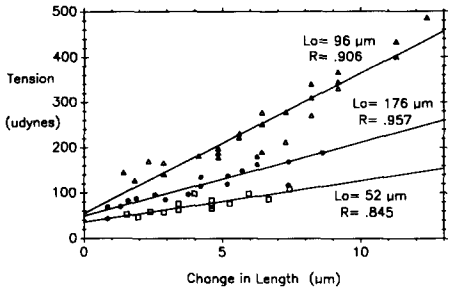


*Figure 2.* Three typical plots of neurite axial tension vs. change in neurite length. Neurite axial tension calculated as described in Materials and Methods is plotted as a function of neurite length change. Each data point represents a single "pull" as shown in Fig. 1. Straight lines were fixed to the data by a least squares fit regression. In all such plots, the slope of the line represents neurite spring constant ($k_1$) and the y-intercept indicates the tension on the neurite with no displacement (neurite rest tension, $T_o$).

rest lengths varied between 34 and 176 µm, and maximum strains varied between 4.1 and 16.6% of the initial rest length. The y-intercept of the length-tension plot represents the tension on the neurite with no displacement (neurite rest tension, $T_o$) and the slope is the neurite spring constant ($k_1$). The observed rest tensions for 82 neurites varied over three orders of magnitude (see Fig. 3) but most neurites exhibited rest tensions in the neighborhood of 35 µdynes, and only one rest tension value was less than zero (-2 µdynes). We found no correlation between neurite length and rest tension. Interestingly, we found a visual cue that correlates to neurite rest tension. A small, roughly spherical bleb in the neurite just proximal to the growth cone is typically associated with low observed rest tensions (1–25 µdynes). This bleb becomes more ovoid in shape in neurites with intermediate rest tensions (25–200 µdynes), disappearing into the neurite body at greater rest tensions. The highest observed tensions (1–3 millidynes) are comparable to those observed in the first cleavage furrow of the echinoderm egg (44).

Neurite spring constants varied over a narrower range than rest tensions. Fig. 4 shows the frequency distribution for spring constants for 75 of the 82 measured neurites. The mean value was 24.4 ± 2.2 (SE) µdynes/µm with 85% of values falling between 5 and 40 µdynes/µm. The seven neurites not included here were those very high tension neurites for which we were unable to obtain accurate spring constant

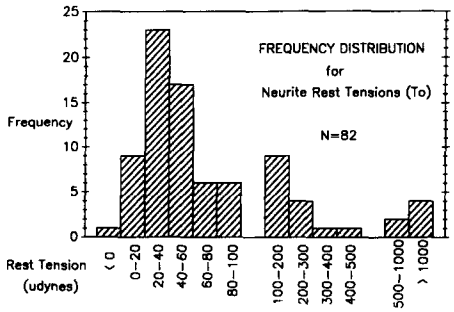


*Figure 3.* Frequency distribution for neurite rest tensions. Summary of results for 82 neurite rest tensions derived from plot intercepts as in Fig. 2.

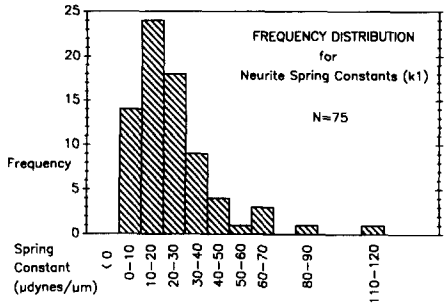


*Figure 4.* Frequency distribution for neurite spring constants. Summary of results for 75 neurite spring constants derived from plot slopes as in Fig. 2.

measurements. There was no significant correlation between spring constant and neurite length or tension.

Experiments involved multiple distensions before and after treatments with anti-cytoskeletal drugs dissolved in DMSO at a final concentration of 0.1%. As control experiments for the effects of DMSO and multiple distensions, we compared length-tension plots before and after treatment with DMSO. We initially deflected neurites various distances in random order to give an untreated reference line. A typical series of 15 to 20 "pulls" on a neurite would last 3 min. DMSO was added to the culture dish to a final concentration of 0.1% and allowed to sit for 10–15 min. The same neurite was then subjected to an additional 15 to 20 pulls of random distensions for comparison with the above. Fig. 5 is typical of these control experiments. Both within and between series of distensions, equal displacements produced nearly identical tension measurements. However, regression lines varied somewhat between pre- and post-DMSO plots producing small differences in rest tensions (y-intercept) and spring constants (slope). In eight experiments, we found that rest tensions after DMSO treatment varied within 50% of their pre-treatment values; the average result was 99.8% of their pre-treatment rest tensions. Similarly, the spring constants averaged 110% of their reference values after DMSO treatment. Measurements from three neurites subjected to two bouts of multiple distensions 15 min apart but without DMSO were indistinguishable from those with added DMSO. We conclude that neither the DMSO carrier nor the distensions themselves significantly affected the neurite mechanical properties measured.

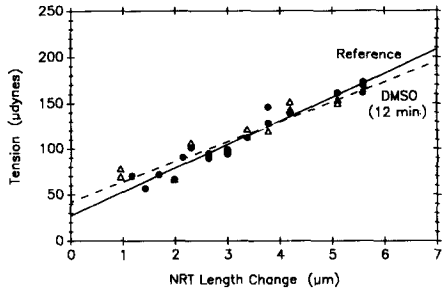


*Figure 5.* Neurite tension as a function of length change before (●) and after (△) addition of 0.1% DMSO (Control Experiment). Neurite axial tension was plotted as a function of neurite length change (see Fig. 2) for two series of displacements on the same neurite.

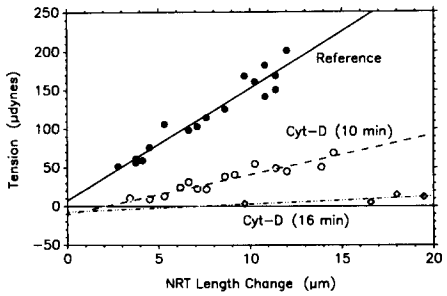


*Figure 6.* Neurite tension as a function of length change before (●), 10 min after (○) and 16 min after (◇) addition of 2 μg/ml cytochalasin D (*Cyt-D*). Neurite axial tension is plotted as a function of neurite length change (see Fig. 2) for three series of displacements on the same neurite. In this trial, growth cone detachment ended the last series of displacements after four pulls. This is neurite No. 6 in Fig. 7.

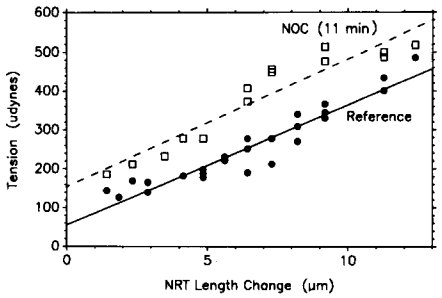


*Figure 8.* Neurite tension as a function of length change before (●) and after (□) addition of 1 μg/ml nocodazole (*NOC*). Neurite axial tension is plotted as a function of neurite length change (see Fig. 2) for two series of displacements on the same neurite. This is neurite No. 8 in Fig. 9.

We tested the effect of the anti-actin drug Cyt-D (16, 45) on the neurite mechanical properties. After a reference series of distensions, neurites were treated with 2 μg/ml Cyt-D for ~10 min. After treatment, additional series of random deflections were carried out on the same neurite. Fig. 6 shows the results of such a Cyt-D experiment, with one pre-treatment plot and two plots showing the effect of Cyt-D at 10 and 16 min. As shown in this figure, the neurite rest tension and spring constant declined with increasing time of drug treatment. However, it was not possible to wait for a steady state value because the neurite behavior became primarily viscous and does not recover from distension. As summarized in Fig. 7, all Cyt-D-treated neurites showed significant declines in rest tension; the maximum rest tension was 31.6% of the reference value. In two cases (including Fig. 6) rest tension values after Cyt-D treatment fell below zero. The average result for all seven neurites was a 114% decline in the initial rest tension, indicating net neurite compression. The neurite spring constants also declined, from a mean 15.2 μdynes/μm to 2.4 μdynes/μm after cytochalasin treatment, 15.8% of the reference value.

We also tested the effect of the anti-microtubule drug NOC (19) on the neurite mechanical properties. After a reference series of deflections, neurites were treated with 1 μg/ml NOC for ~10 min followed by an additional series of random deflections on the same neurite. Fig. 8 shows the results of a typical NOC experiment, with one pre-treatment plot and one plot showing the effect of NOC at 11 min. As summarized in Fig. 9, all NOC treated neurites showed an increase in rest tension ranging from 153 to 560% of the reference rest tension with an average value of 282%. These values appeared to be short lived plateaus; all neurites eventually retracted in response to the increased tension. However the neurite spring constants did not show a consistent change: four went up, two went down and two remained the same. The shift in the mean was negligible, going from a reference value of 20.5 μdynes/μm to 20.0 μdynes/μm in the drug treated neurites.

### *Surface Active Agents Cause Neurite Retraction*

PC-12 cells are commonly grown on collagen or polycationic surfaces (23). We reasoned that the tensile support provided by attachment to polylysine-treated surfaces could be eliminated by neutralizing polylysine with a polyanion, thus allowing rest tension to cause retraction. Indeed, 81% of PC-12 neurites grown on polylysine treated tissue culture plates retract after 30-min treatment with 1% polyaspartate (Table I). This polyaspartate treatment caused only 4% retraction of neurites grown on a collagen-treated substratum, while treatment with 0.25% trypsin caused 92% retraction. Addition of 2 μg/ml Cyt-D rescued most polylysine-grown neurites from polyaspartate induced retraction. Similar cytochalasin effects have been noted for other methods of inducing neurite retraction (31, 49).

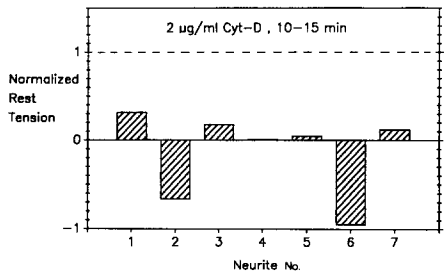


*Figure 7.* Summary of the effect of cytochalasin D (*Cyt-D*) on neurite rest tension. The effect of Cyt-D on rest tension is plotted for each of seven neurites. The initial rest tension for each neurite is normalized to 1 and the graph shows the relative change for that neurite's rest tension after 10-15 min exposure to Cyt-D.

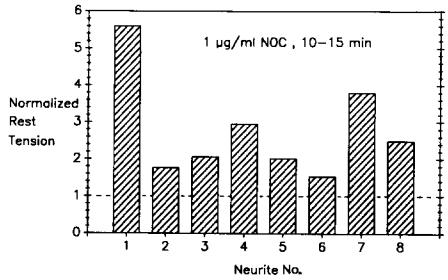


*Figure 9.* Summary of the effect of nocodazole (*NOC*) on neurite rest tension. The effect of NOC on neurite rest tension is plotted for each of eight neurites. The initial rest tension for each neurite was normalized to 1 and the graph shows the relative change for that neurite's rest tension after 10–15 min exposure to NOC.

### *Microtubule Depolymerization is Associated with Neurite Retraction*

Retraction also has the effect of shifting tensile support (compression) to internal elements of the neurite. We wished to determine whether this would affect MT stability as predicted by thermodynamics (11, 25). The effect of polyaspartate treatment on microtubule assembly with and without retraction was tested by measuring the pools of soluble and polymerized tubulin by quantitative immunoblotting method similar to that of Drubin et al. (20). Cultures were treated with surface active agents as in Table I and then detergent extracted to produce samples containing the soluble (Triton extract) and polymerized (SDS extract) pools of tubulin. Extractions were carried out such that equal cell numbers were represented in equal volumes of both Triton and SDS extracts. Aliquots of Triton and SDS extracts from the same dish were subjected to electrophoresis, transferred to nitrocellulose and reacted with a monoclonal antibody to beta tubulin (kind gift of Dr. David Asai) as described in Materials and Methods. The amount of beta tubulin in the aliquots was measured by scanning the blots with a soft laser densitometer equipped with a numerical integrator for the areas of the peaks. Calibration curves for immunoblotting phosphocellulose purified tubulin from beef brain from 0.5 to 5.5 μg (Fig. 10) indicate a linear response to beta tubulin. Fig. 11 shows a typical immunoblot of Triton and SDS extracts (soluble and polymerized pools) from PC-12 cells under various experimental treatments. Table II summarizes the measurements of soluble and polymerized tubulin pools from five separate experiments using the same experimental treatments as in Table I. Untreated cells on polylysine surfaces had ~1/3 of the tubulin in the soluble fraction and the remaining 2/3 in the polymer pool. After neurite retraction induced by polyaspartate, the soluble:polymerized tubulin ratio generally became 1:1 but in one experiment became nearly 4:1. A shift in the soluble:polymerized tubulin ratio was not observed in cultures treated with polyaspartate but grown on collagen treated surfaces. Polyaspartate treatment also had no effect on the ratio of soluble to polymerized tubulin in cultures treated with anti-actin drugs, cytochalasin D or EHNA (46).

The 1:2 ratio of soluble to polymerized tubulin in control cultures of extended neurites is lower than that reported by Drubin et al. (20) for PC-12 cells, but are in good agreement with the values of Morris and Lasek (40) from squid axon. This is possibly due to the method of Drubin et al. of calculating the soluble pool by subtraction from total pool measurements made on separate cultures; we, like Morris and Lasek, measured soluble and polymerized pools from the same cells.

## *Discussion*

We found that growing neurites of PC-12 behaved as simple elastic solids for short duration distensions (2–3). That is, we consistently found a linear relationship between applied force (axial tension) and the induced length change, and a high degree of reproducibility in measured force in multiple trials of the same distension (Fig. 2). In the presence of anti-cytoskeletal drugs, the linear regression coefficients decreased somewhat. This may reflect time dependent changes in spring constants during drug treatment of the neurites. As expected from observations of other cells (27, 38, 42, 43), neurites behave viscoelastically under longer duration distensions.

The majority (67%) of our measurements reported in Figs. 3 and 4 and all of our drug experiments were on isolated, nonbranching neurites with active, filopodia bearing growth cones attached to the dish. We observed 23 such neurites for 30 min and found an average rate of elongation of 5.3 μm/h, supporting the premise that this population is in an active growth phase. The remaining tension measurements were on neurites that terminated on other cells (23%), those that did not have visible filopodial activity (9%) and branched neurite segments (1%). Measurements from these neurites were

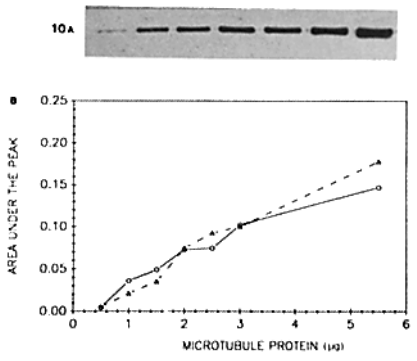


*Figure 10.* Immunoblot of MTP purified from beef brain. Phosphocellulose purified tubulin of concentrations from 0.5 μg to 3.0 μg in 0.5-μg increments and a 5.5-μg sample were subjected to electrophoresis in adjoining lanes of a 10% SDS polyacrylamide gel. (*a*) Photograph of nitrocellulose paper after immunoblotting. (*b*) Integrated area under the beta tubulin peaks as determined by LKB 2222 laser densitometer as a function of applied MTP mass. This graph shows the results for two separate experiments using arbitrary units for area values.

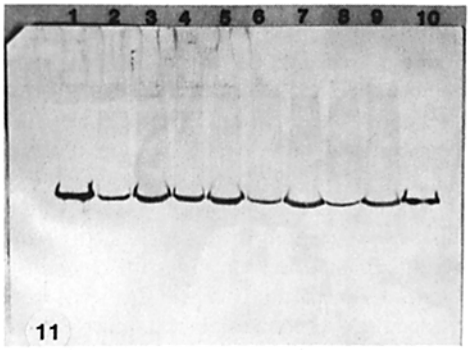


*Figure 11.* Immunoblot of PC-12 extracts under experimental conditions. (Lane *1*) 3.0 μg brain tubulin. (Lanes *2* and *3*) Soluble and polymerized pools respectively from untreated culture grown on polylysine. (Lanes *4* and *5*) Soluble and polymerized pools respectively from cultures grown on polylysine whose neurites had retracted in response to 1% polyaspartate treatment. (Lanes *6* and *7*) soluble and polymerized pools respectively from cultures grown on polylysine, treated with 2.0 μg/ml Cyt-D and polyaspartate. (Lanes *8* and *9*) soluble and polymerized pools respectively from cultures grown on polylysine and treated with 0.2 mM EHNA and 1% polyasparate. (Lane *10*) 1.0 μg brain tubulin. This blot is identified as experiment No. 1 in Table II.

*Table II. Western Blot Analysis of Soluble and Polymerized Tubulin Pools*

| Experiment no. | Surface | Treatment | Neurites | Soluble pool* | Polymerized pool* |
|---|---|---|---|---|---|
| | | | | % | % |
| 1 | PolyLys | None | Extended | 21 | 79 |
| 2 | PolyLys | None | Extended | 33 | 67 |
| 3 | PolyLys | None | Extended | 33 | 67 |
| 4 | PolyLys | None | Extended | 34 | 66 |
| 5 | PolyLys | None | Extended | 36 | 64 |
| 1 | PolyLys | PolyAsp | Retracted | 50 | 50 |
| 2 | PolyLys | PolyAsp | Retracted | 52 | 48 |
| 3 | PolyLys | PolyAsp | Retracted | 78 | 22 |
| 4 | PolyLys | PolyAsp | Retracted | 54 | 46 |
| 5 | PolyLys | PolyAsp | Retracted | 47 | 53 |
| 2 | Collagen | PolyAsp | Extended | 30 | 70 |
| 3 | Collagen | PolyAsp | Extended | 33 | 67 |
| 4 | Collagen | PolyAsp | Extended | 33 | 67 |
| 5 | Collagen | PolyAsp | Extended | 37 | 63 |
| 1 | PolyLys | PolyAsp + Cyt-D | Extended | 34 | 66 |
| 1 | PolyLys | PolyAsp + EHNA | Extended | 35 | 65 |
| 5 | PolyLys | PolyAsp + Cyt-D | Extended | 36 | 64 |

* The soluble pool fraction was calculated as the peak area of the beta tubulin band from the Triton extract of a culture dish divided by the sum of the peak areas from both Triton and SDS extracts of the same dish. Similarly, the polymerized pool fraction was calculated as the peak area of the beta tubulin band from the SDS extract divided by the sum of the peak areas from both extracts of the same dish.

indistinguishable from the majority of tension measurements. The most highly selected neurites were those which survived NOC treatment. Most PC-12 neurites retract after treatment with NOC (24, 31) but this tendency can be decreased (3, 30) by allowing neurite outgrowth for periods longer than the 24 h used previously (24, 31). Approximately 30% of the cells regrown for 2–3 d and subjected to reference distensions remained extended long enough after NOC treatment to allow an additional series of distensions.

Direct mechanical measurements reported here confirm the hypothesis that neurites are under tension (5, 31). The rest tension values were greater than zero in all but 1 of 82 growing neurites (Figs. 2 and 3). Clearly, the maintenance of this tension requires structural support. Our ability to measure a net tension in the highly asymmetric neurite at its "rest" length indicates that there is some tensile element in the neurite itself, and that this tension is at least partially supported externally, i.e., by compression of the dish. We are unable to interpret the wide range of observed neurite rest tensions (Fig. 3) at this time. However, experiments in progress should enable us to determine whether rest tension is related to some other variable such as neurite circumference, cortical actin network cross sectional area (Albrecht-Buhler, G., personal communication), total cross sectional area (5) and/or rate of elongation (6).

Neurite rest tensions may be manifestations of "surface forces" or "cortical tensions" observed by others in a variety of cell types (2, 14, 27, 38, 42, 43, 48). Cortical tension may be the passive result of an osmotic force, an occasionally activated "motor" (9) or could be actively generated continuously within the cortical actin network (2, 9). Alternatively, the neurite tension may be the passive result of tension generated by the growth cone (7, 10, 12, 34, 35, 54). For a number of reasons we assume the measured tension is held passively. Previous results indicate that combined inhibitors of glycolysis and oxidative phosphorylation do not affect neurite retraction in PC-12 (31). The majority of evidence in neurons supports a pulling growth cone and we are unaware of studies suggesting continuously generated cortical force in neurites. Also, the assumption of continuously generated tension requires a number of ad hoc assumptions, not needed for passive tension models, to explain the tension changes after drug treatments. Passive tension allows us to interpret the effect of drugs by a simple force balance between elastic cytoskeletal elements; actin filaments and MTs being measurably elastic in vitro (39, 60). Not withstanding, experiments are planned to test whether neurite tension is passive or continuously generated within the neurite.

Direct mechanical measurements demonstrate (Figs. 6 and 7) that Cyt-D significantly reduces neurite rest tension. This indicates that anti-actin drug-sensitive elements are in tension. We presume the drug-sensitive structure correlates with the highly cross-linked, actin-rich subplasmalemmal region of neurites (26, 47). Addition of Cyt-D disrupts actin networks in vivo (16, 45) dissipating tension in the network. If MTs are providing internal compressive support (31), their depolymerization should transfer additional tension support to the dish causing an increase in rest tension. Indeed, our measurements before and after depolymerization of MTs by NOC (19) demonstrate a significant increase in neurite rest tension in the presence of NOC (Figs. 8 and 9), supporting our claim that MTs are in compression and lending support to our previous claim (31) that NOC causes neurite retraction by increasing tension. The existence of an internal compressive support in the neurite is also suggested by the two cases where neurite rest tension fell below zero (and became a positive compression) in the presence of Cyt-D. Under conditions of stationary neurite attachment to a stationary sub-

strate, the change in neurite force from net tension to net compression indicates that some internal element is under compression. Based on changes in cell shape caused by cytoskeletal drugs, chick embryo fibroblasts grown in collagen matrix appear to have a similar complementary force interaction within the actin and MT elements of their cytoskeleton (52).

The effects of the anticytoskeletal drugs were quantitatively inconsistent. The apparent tension in the actin network (the tension measured in the presence of NOC) was greater than the sum of the apparent compression in the MTs (measured in the presence of cytochalasin) and the compression of the dish (the rest tension). The explanation we favor is that the surface interactions between actin and MTs (26, 47) provide a stabilization, i.e., a surface compression, whose magnitude is the difference observed above. Such an effect was expected and a formal model for the tension and compression relationships within the cytoskeleton includes a term for this force (11). An alternative explanation that we cannot rule out at present is that depolymerizing MTs causes a net increase in tension generated by the actin network.

The observed complementary force interaction between a surrounding tensile network and an internal compressive support, similar to the "tensegrity" architecture of Buckminster Fuller (21), has also been proposed by Ingber and others to explain cell shape (28, 29). Tension in such architectures has the counter-intuitive effect of stabilizing elongated forms such as masts (21). Axons resemble tensegrity structures (21) in their very large ratio of length to cross-sectional area, their elasticity and strength, and the finding that the putatively tensile actin network is continuous beneath the plasma membrane while the compressive MTs are arrayed as discrete, internal fascicles (26, 47).

In principle, alteration of the force balance between cytoskeletal elements of the neurite could regulate their assembly. For example, increases in MT compression would favor depolymerization (11, 25). Polyaspartate treatment apparently disturbs the force balance in the neurite causing retraction. The retraction of neurites in response to polyaspartate treatment must therefore be due either to a directly induced increase in tension or to elimination of some existing support for tension. The relative lack of effect of polyaspartate treatment on neurites cultured on collagen argues against a direct increase in force, suggesting rather that polyaspartate induced retraction by charge neutralization causing the release of neurite adhesion. This treatment shifted compressive support, formerly on the dish, onto internal elements. Because retraction is complete, while extensions were only 10% of the neurite length, we reasoned that MT depolymerization in response to increased compression would be easier to measure than MT assembly in response to elongation. Also, we do not presently have a technique for extending a population of neurites to measure MT assembly. Polyaspartate treatments were coupled with quantitative immunoblotting of soluble and polymerized tubulin pools to test the effect of increased internal compression on the microtubules. We observed that neurite length (retracted or extended) affects microtubule polymerization. Cells with extended neurites, under a variety of treatments, had a soluble:polymerized tubulin ratio of 1:2. However after polyaspartate induced neurite retraction, the soluble:polymerized tubulin ratio generally became 1:1 and in one experiment nearly reached 4:1. Reduction in rest tension with cytochalasin or EHNA (another actin-disrupting drug, 46) rescues cells from polyaspartate induced depolymerization and retraction. The lack of effect of polyaspartate treatment on retraction or the soluble:polymerized tubulin ratio of collagen-grown cells indicates that polyaspartate does not have a direct effect on tubulin polymerization independent of retraction. These results suggest that the alteration in the soluble:polymerized tubulin ratio in polyaspartate treated cultures grown on polylysine has the same cause as neurite retraction: alteration in the force balance. We postulate the increase in microtubule compression, due to the shift of tensile support to internal elements after release of adhesion, shifted the MT assembly equilibrium toward disassembly (11, 25). However, we cannot exclude the possibility that an unknown chemical response to retraction or cell shape change, e.g. $Ca^{++}$ influx, is responsible for the microtubule depolymerization observed. Effects due to force per se and to secondary effects of movement will be difficult to differentiate in living cells because of the close relationship of force to movement. However, we are presently working to distinguish these possibilities.

Our data are consistent with the hypothesis that complementary force interactions integrate MT assembly with the advance of the growth cone (31). In one widely accepted elongation model, axons are pulled out by tension exerted by the growth cone (7, 10, 12, 34, 54). We postulate the growth cone advance shifts a small amount of tension onto the environment, relieving some of the compressive force on MTs, and thus lowering their critical concentration for assembly (11, 25). Tubulin subunits, which had been in equilibrium with the compressed polymer, now add into the polymer until the MT elongates sufficiently to again come under equilibrium compression. This predicts that diminution of neurite tension by cytochalasin should cause MT assembly. Treatment of Aplysia growth cones with cytochalasin causes a marked extension of MTs, although it is not clear that the extension is due to additional assembly (20*a*). The postulated complementary force interaction model is also consistent with recent data suggesting axonal elongation without motile activity of the growth cone (37) and/or growth cone advance via a pushing mechanism (22). Under these conditions, we postulate that MTs are pushing out the neurite using the energy of polymerization as the driving force. However, MT assembly would still depend on the balance of free energy between MT polymers under compression and in the tubulin subunit pool. This mechanism tends, depending on the details of pushing and of growth cone attachment, to produce curvy elongation of neurites because pushing within the flexible neurite is similar to pushing on a rope. Indeed, outgrowth of chick sensory neurites in the presence of cytochalasin (actin destabilization, presumably little or no tension) is markedly curvy (37), in contrast to undrugged, straight, growth by this cell type. Neurites grown in the presence of both taxol (a potent stimulator of MT assembly) and cytochalasin, where growth is likely to be due to MTs pushing out, are also very curvy (35, 51). These results support the net compression possibilities of our complementary force model.

We wish to thank Bruce Nicklas for hospitality in his laboratory and his help in learning the use of glass needles for the measurement of tension. We are indebted to David Asai for his generous gifts of tubulin antibody and to Mike

Mullins for helpful discussions on immunoblotting. We also thank Guenter Albrecht-Buhler for a stimulating discussion.

This work was supported by grants GM 36894 from National Institutes of Health (NIH) and National Science Foundation (NSF) grant BNS 8401904. Purchase of a laser densitometer was made possible by a grant from the Michigan State University Biotechnology Research Center, we also thank Christin Carter-Su of the University of Michigan for access to her laser densitometer early in this work.

### *References*

1. Alberts, B. M., D. Bray, J. Lewis, M. Raff, K. Roberts, and J. D. Watson. 1983. Molecular Biology of the Cell. New York: Garland Publishing. 549.
2. Albrecht-Buhler, G. 1987. Role of cortical tension in fibroblast shape and movement. *Cell Motil. Cytoskeleton.* 7:54–67.
3. Aletta, J. M., and L. A. Greene. 1987. Sequential phosphorylation of chartin microtubule-associated proteins is regulated by the presence of microtubules. *J. Cell Biol.* 105:277–290.
4. Black, M. M., and R. J. Lasek. 1980. Slow components of axonal transport: two cytoskeletal networks. *J. Cell Biol.* 86:616–622.
5. Bray, D. 1979. Mechanical tension produced by nerve cells in tissue culture. *J. Cell Sci.* 37:391–410.
6. Bray, D. 1984. Axonal growth in response to experimentally applied tension. *Dev. Biol.* 102:379–389.
7. Bray, D. 1987. Growth cones: do they pull or are they pushed? *Trends Neurosci.* 10:431–434.
8. Bray, D., C. Thomas, and G. Shaw. 1978. Growth cone formation in cultures of sensory neurons. *Proc. Natl. Acad. Sci. USA.* 75:5226–5229.
9. Bray, D., and J. G. White. 1988. Cortical flow in animal cells. *Science (Wash. DC).* 239:883–888.
10. Bunge, M. B., M. I. Johnson, and V. J. Argiro. 1983. Studies of regenerating nerve fibers and growth cones. *In* Spinal Cord Reconstruction. C. Kao, R. P. Bunge, and P. J. Reiner, editors. Raven Press, New York. 99–120.
11. Buxbaum, R. E., and S. R. Heidemann. 1988. A thermodynamic model for microtubule assembly during axonal growth. *J. Theor. Biol.* In press.
12. Campenot, R. B. 1984. The regulation of nerve fiber length by intercalated elongation and retraction. *Dev. Brain Res.* 20:149–154.
13. Cande, W. Z., J. Snyder, D. Smith, K. Summers, and J. R. McIntosh. 1974. A functional mitotic spindle prepared from mammalian cells in culture. *Proc. Natl. Acad. Sci. USA.* 71:1559–1563.
14. Cole, K. S. 1932. Surface forces of the Arbacia egg. *J. Cell Comp. Physiol.* 1:1–19.
15. Corvaja, N., A. DiLuzio, S. Biocca, A. Cattaneo, and P. Callisano. 1982. Morphological and ultrastructural changes in PC 12 pheochromocytoma cells induced by combined treatment with taxol and NGF. *Exp. Cell Res.* 142:385–395.
16. Cooper, J. A. 1987. Effects of cytochalasin and phalloidin on actin. *J. Cell Biol.* 105:1473–1478.
17. Daniels, M. 1975. The role of microtubules in the growth and stabilization of nerve fibers. *Ann. NY Acad. Sci.* 253:535–544.
18. Darnell, J., H. Lodish, and D. Baltimore. 1986. Molecular Cell Biology. Scientific American Books, New York. 771.
19. DeBrabander, M., G. Guens, F. Van de Viere, F. Thone, F. Aerts, L. Desplanter, J. DeCree, and M. Borgers. 1977. The effects of R 17934, a new antimicrotubular substance, on the ultrastructure of neoplastic cells in vivo. *Eur. J. Cancer.* 13:511–528.
20. Drubin, D. G., S. C. Feinstein, E. M. Shooter, and M. W. Kirschner. 1985. Nerve growth factor-induced neurite outgrowth in PC 12 cells involves the coordinate induction of microtubule assembly and assembly-promoting factors. *J. Cell Biol.* 101:1799–1807.

20a. Forscher, P., and S. J. Smith. 1988. Actions of cytochalasins on the organization of actin filaments and microtubules in a neuronal growth cone. *J. Cell Biol.* In press.

21. Fuller, R. B. 1961. Tensegrity. *Portfolio and Artnews Annual.* 4:112–127.
22. Goldberg, D. J., and D. W. Burmeister. 1986. Stages in axon formation: observations of growth of Aplysia axons in culture using video-enhanced-contrast-differential interference microscopy. *J. Cell Biol.* 103:1921–1931.
23. Greene, L., and A. S. Tischler. 1982. PC 12 Pheochromocytoma cultures in neurobiological research. *Adv. Cell. Neurobiol.* 3:373–414.
24. Heidemann, S. R., H. C. Joshi, A. Shechter, J. R. Fletcher, and M. Bothwell. 1985. Synergistic effects of cyclic AMP and nerve growth factor on neurite outgrowth and microtubular stability of PC-12 cells. *J. Cell Biol.* 100:916–927.
25. Hill, T. L., and M. W. Kirschner. 1982. Bioenergetic and kinetics of microtubule and actin filament assembly-disassembly. *Int. Rev. Cytol.* 78: 1–125.
26. Hirokawa, N. 1982. Cross linker system between neurofilaments, microtubules, and membranous organelles revealed by the quick freeze, deep etching method. *J. Cell Biol.* 94:129–142.
27. Hiramoto, Y. 1963. Mechanical properties of sea urchin eggs. *Exp. Cell Res.* 32:59–75.
28. Ingber, D. E., and J. D. Jamieson. 1985. Cells as tensegrity structures: architectural regulation of histodifferentiation by physical forces transduced over basement membrane. *In*: Gene Expression during Normal and Malignant Differentiation. L. C. Anderson, C. G. Gahmberg, and P. Ekblom, editors. Academic Press, Orlando. 13–32.
29. Ingber, D. E., and J. Folkman. 1988. Tension and compression as basic determinants of cell form and function: Utilization of a cellular tensegrity mechanism. *In* Cell Shape: Determinants, Regulation and Regulatory Role. W. D. Stein and F. Bronner, editors. Academic Press, Orlando. In Press.
30. Jacobs, J. R., and J. K. Stevens. 1986. Experimental modification of PC12 neurite shape with the microtubule-depolymerizing drug nocodazole: a serial electron microscopic study of neurite shape control. *J. Cell Biol.* 103:907–916.
31. Joshi, H. C., D. Chu, R. E. Buxbaum, and S. R. Heidemann. 1985. Tension and Compression in the Cytoskeleton of PC 12 Neurites. *J. Cell Biol.* 101:697–705.
32. Kolega, J. 1986. Effects of mechanical tension on protrusive activity and microfilament and intermediate filament organization in an epidermal epithelium in culture. *J. Cell Biol.* 102:1400–1411.
33. Laemmli, U. K. 1970. Cleavage of structural proteins during the assembly of the head of bacteriophage T4. *Nature (Lond.).* 227:680–685.
34. Landis, S. C. 1983. Neuronal growth cones. *Annu. Rev. Physiol.* 45: 567–580.
35. Letourneau, P. C., T. A. Shattuck, and A. H. Ressler. 1987. "Pull" and "push" in neurite elongation: observations on the effects of different concentrations of cytochalasin B and taxol. *Cell Motil. Cytoskeleton.* 8: 193–209.
36. Lintilhac, P. M., and T. B. Vesecky. 1984. Stress-induced alignment of division plane in plant tissues grown in vitro. *Nature (Lond.).* 307: 363–364.
37. Marsh, L., and P. C. Letourneau. 1984. Growth of neurites without filopodial or lamellipodial activity in the presence of cytochalasin B. *J. Cell Biol.* 99:2061–2067.
38. Mitchison, J. M., and M. M. Swann. 1954. The mechanical properties of the cell surface. I. The cell elastimeter. *J. Exp. Biol.* 31:443–460.
39. Mizushima-Sugano, J., T. Maeda, and T. Miki-Nomura. 1983. Flexural rigidity of singlet microtubules estimated from statistical analysis of their contour lengths and end-to-end distances. *Biochem. Biophys. Acta.* 755: 257–262.
40. Morris, J. R., and R. J. Lasek. 1982. Stable polymers of the axonal cytoskeleton: the axoplasmic ghost. *J. Cell Biol.* 92:192–198.
41. Nicklas, R. B. 1983. Measurements of the force produced by the mitotic spindle in anaphase. *J. Cell Biol.* 97:542–548.
42. Pasternak, C., and E. L. Elson. 1985. Lymphocyte mechanical response triggered by cross-linking surface receptors. *J. Cell Biol.* 100:860–872.
43. Peterson, N. O., W. B. McConnaughey, and E. L. Elson. 1982. Dependence of locally measured cellular deformability on position on the cell, temperature and cytochalasin B. *Proc. Natl. Acad. Sci. USA.* 79:5327–5331.
44. Rappaport, R. 1967. Cell division: direct measurement of maximum tension exerted by furrow of echinoderm eggs. *Science (Wash. DC).* 167: 1241–1242.
45. Schliwa, M. 1982. Action of cytochalasin D on cytoskeletal networks. *J. Cell Biol.* 92:79–91.
46. Schliwa, M., R. M. Ezzell, and U. Euteneuer. 1984. Erythro-9-[3-(2 hydroxynonyl)] adenine is an effective inhibitor of cell motility and actin assembly. *Proc. Natl. Acad. Sci. USA.* 81:6044–6048.
47. Schnapp, B. J., and T. S. Reese. 1982. Cytoplasmic structure in rapid frozen axons. *J. Cell Biol.* 94:667–679.
48. Schroeder, T. E. 1981. The origin of cleavage in dividing eggs. *Exp. Cell Res.* 134:231–240.
49. Solomon, F., and M. Magendantz. 1981. Cytochalasin separates microtubule disassembly from loss of asymmetrical morphology. *J. Cell Biol.* 89:157–161.
50. Solomon, F., M. Magendantz, and A. Salzman. 1979. Identification with microtubules of one of the microtubule-associated proteins. *Cell.* 18: 431–438.
51. Spero, D. A., and F. J. Roisen. 1985. Neuro-2a neuroblastoma cells form neurites in the presence of taxol and cytochalasin D. *Dev. Brain Res.* 23: 155–159.
52. Tomasek, J. J., and E. D. Hay. 1984. Analysis of the role of microfilaments and microtubules in acquisition of bipolarity and elongation of fibroblasts in hydrated collagen gels. *J. Cell Biol.* 99:536–549.
53. Trinkaus, J. P. 1984. Cells Into Organs. 2nd Edition. Prentice Hall Inc., Englewood Cliffs, NJ.
54. Trinkaus, J. P. 1985. Further thoughts on directional cell movement during morphogenesis. *J. Neurosci. Res.* 13:1–19.
55. Vandenburgh, H. H. 1982. Dynamic mechanical orientation of skeletal myofibers in vitro. *Dev. Biol.* 93:438–443.
56. Weingarten, M. W., M. Suter, D. Littman, and M. W. Kirschner. 1974. Properties of the depolymerization products of microtubules from mammalian brain. *Biochemistry.* 13:5529–5537.
57. Weiss, P. 1941. Nerve Pattern: The mechanics of nerve growth. *Growth.* 5(Suppl. Third Growth Symp.):163–203.

58. Williams, R. C., and H. W. Detrich. 1979. Separation of tubulin from microtubule-associated proteins on phosphocellulose. Accompanying alterations in concentrations of buffer components. *Biochemistry.* 18: 2499–2503.
59. Yamada, K. M., B. S. Spooner, and N. K. Wessels. 1970. Axon growth: role of microfilaments and microtubules. *Proc. Natl. Acad. Sci. USA.* 66: 1206–1212.
60. Yanagida, T., and F. Oosawa. 1978. Polarized fluorescence from e-ADP incorporated into F-actin in a myosin free single fiber: conformation of F Actin and changes induced in it by heavy meromyosin. *J. Mol. Biol.* 126:507–524.